

Supporting Information

Two-Photon Absorption in a Series of 2,6-Disubstituted BODIPY Dyes

Leonardo W. T. Barros,[‡] Thiago A. S. Cardoso,[‡] Angela Bihlmeier,^{*,#} Danny Wagner,^{†,||} Dominik K. Kölmel,[†] Anna Hörner,^{†,|} Stefan Bräse,^{†,||} Carlos H. Brito Cruz,[‡] and Lazaro A. Padilha^{*,‡}

[‡]Instituto de Física “Gleb Wataghin”, Universidade Estadual de Campinas, C. P. 6165, 13083-970 Campinas, Sao Paulo, Brazil

[#]Institute of Physical Chemistry, Karlsruhe Institute of Technology, 76131 Karlsruhe, Germany

[†]Institute of Organic Chemistry, Karlsruhe Institute of Technology, 76131 Karlsruhe, Germany

^{||}Institute of Toxicology and Genetics, Karlsruhe Institute of Technology, 76344 Eggenstein-Leopoldshafen, Germany

Light Technology Institute, Karlsruhe Institute of Technology, 76131 Karlsruhe, Germany

Contents

1. General Information
2. Experimental Procedures and Characterization
3. Linear and Nonlinear Absorption Studies
4. Computational Studies
5. References

1. General Information

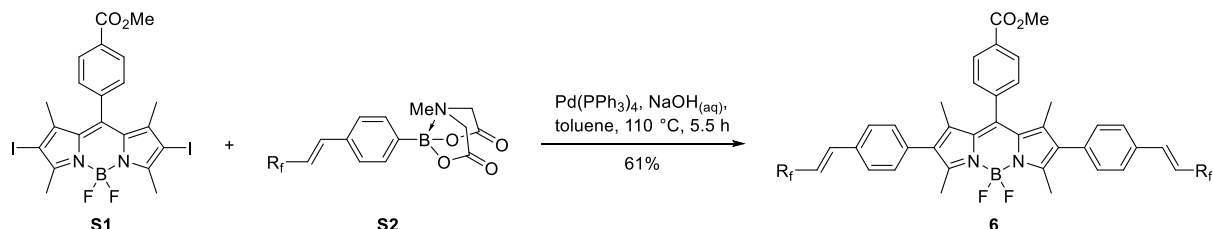
All chemicals were used as received. All reactions were carried out under stirring. Reactions under inert gas were carried out in flasks equipped with septa under argon (supplied by using a standard manifold with vacuum and argon lines). Analytical TLC was performed on MERCK ready-to-use plates with silica gel 60 (F254). Column chromatography: MERCK silica gel 60, 0.04–0.063 mm. IR spectra were recorded by using FT-IR Bruker ALPHA-T spectrometer. The samples were measured by using the attenuated total reflexion (ATR) technique. The transmission intensities of the bands were characterized as follows: s = strong (11–40%), m = medium (41–70%), w = weak (71–90%), vw = very weak (91–100%) transmission. NMR spectra were recorded at 25 °C by using Bruker AM 400 (400 (1H), 376.5 (19F) and 100 MHz (13C)) spectrometer. All spectra are referenced to tetramethylsilane as standard ($\delta = 0$ ppm) by using the signals of the solvent:

CDCl_3 : 7.26 ppm (CHCl_3) or 77.16 ppm ($^{13}\text{CDCl}_3$)

The spectra were analyzed according to first order. Multiplicities of the signals are described as follows: s = singlet, d = doublet, t = triplet, q = quartet, dt = doublet of triplet, m = multiplet. Coupling constants (J) are given in Hz. Multiplicities in the ^{13}C NMR spectra were determined by DEPT (distortionless enhancement by polarization transfer) measurements. Perfluorinated carbon atoms were not analyzed by ^{13}C NMR spectroscopy due to their weak signals.

2. Experimental Procedures and Characterization

Scheme S1. Synthesis of BODIPY dye **6**. $R_f = (\text{CF}_2)_5\text{CF}_3$.



4,4-Difluoro-8-(4-(methoxycarbonyl)phenyl)-1,3,5,7-tetramethyl-2,6-bis(4-((*E*)-1*H*,2*H*-perfluorooct-1-en-1-yl)phenyl)-4-bora-3a,4a-diaza-*s*-indacene (**6**):

BODIPY dye **S1**¹ and fluororous boronic MIDA ester **S2**² were synthesized as previously reported. BODIPY dye **S1** (50.0 mg, 78.9 μmol), fluororous boronic acid MIDA ester **S2** (100 mg, 174 μmol) and $\text{Pd}(\text{PPh}_3)_4$ (9.1 mg, 7.89 μmol) were added to a vial. The vial was capped with a rubber septum and then purged with argon. Afterwards 1.60 mL toluene (degassed by bubbling with argon for 30 min) was added via a syringe and stirred for 10 min at room temperature. Then, 435 μL aq. NaOH (3.0 M, degassed by bubbling with argon for 30 min) was added and the mixture was heated to $110\text{ }^\circ\text{C}$ for 5.5 h. After cooling to ambient temperature, the mixture was partitioned between 20 mL dichloromethane and 10 mL water. The organic layer was separated and evaporated under reduced pressure. The crude product was purified by using column chromatography (eluent cyclohexane/ CH_2Cl_2 3:1 \rightarrow 2:1) to give a red solid (58.5 mg, 61%).

^1H NMR (400 MHz, CDCl_3): $\delta = 1.30$ (s, 6H), 2.55 (s, 6H), 3.97 (s, 3H), 6.23 (dt, $J(\text{H,H}) = 15.9$ Hz, $J(\text{H,F}) = 12.1$ Hz, 2H), 7.15–7.24 (m, 6H), 7.48 (d, $J(\text{H,H}) = 8.2$ Hz, 2H), 7.52 (d, $J(\text{H,H}) = 8.1$ Hz, 4H), 8.21 (d, $J(\text{H,H}) = 8.2$ Hz, 2H); ^{13}C NMR (100 MHz, CDCl_3): $\delta = 12.9$ (CH_3), 13.5 (CH_3), 52.4 (CH_3), 114.3 (t, $J(\text{C,F}) = 24$ Hz, CH), 127.7 (C), 128.4 (CH), 130.6 (CH), 130.7 (CH), 131.0 (C), 131.1 (C), 132.4 (C), 133.2 (C), 135.5 (C), 139.1 (C), 139.2 (CH), 140.0 (C), 141.0 (C), 154.9 (C), 166.4 (C); ^{19}F NMR (376.5 MHz, CDCl_3): $\delta = -145.9$ (q, $J(\text{F,B}) = 32$ Hz, BF_2), -126.1 (m, $2 \times \text{CF}_2$), -123.1 (m, $2 \times \text{CF}_2$), -122.8 (m, $2 \times \text{CF}_2$), -122.5 (m, $2 \times \text{CF}_2$), -111.0 (t, $J(\text{F,F}) = 12$ Hz, $2 \times \text{CF}_2$), -80.7 (t, $J(\text{F,F}) = 10$ Hz, $2 \times \text{CF}_3$); IR (ATR): $\tilde{\nu}$ (cm^{-1}) = 2929 (vw), 1721 (w), 1656 (w), 1610 (vw), 1534 (m), 1466 (w), 1393 (w), 1365 (w), 1317 (w), 1277 (w), 1233 (m), 1174 (s), 1141 (m), 1105 (m), 1067 (m), 1010 (m), 979 (m), 923 (w), 841 (w), 820 (w), 789 (w), 738 (m), 707 (m), 641 (m), 566 (m), 511 (m).

3. Linear and Nonlinear Absorption Studies

Linear absorption for all dyes was measured using a Cary-300 UV-Vis spectrometer and the two-photon absorption was measured using the two-photon excited fluorescence technique (2PF).³

Briefly, for the 2PF experiments, the samples are prepared at high concentration, typically from 100's μM to 1.0 mM, in a 1 mm spectroscopy grade cuvette. The excitation is chosen, for photon energies below the $S_0 \rightarrow S_1$ transition energy, from a femtosecond tunable laser system (Ti:sapphire amplifier and optical parametric amplifiers). Upon the excitation, the emitted fluorescence is collected and detected by a home-built spectrofluorometer. In order to correct the emitted signal by the sample reabsorption (which is due to the small Stokes shift), low concentration samples (typically 1–10 μM) are prepared and their emissions are used to correct the high concentration data.

To obtain the absolute 2PA cross section for the investigated samples, we have used rhodamine B in methanol as our reference sample.⁴

4. Computational Studies

Details of the calculations

All TDDFT calculations for dyes **1**, **4–5** as well as for the simplified structures of dyes **2** and **3** ($R_f = CF_3$) were carried out on B3LYP⁵/def2-TZVP⁶ optimized geometries as described in our previous work.² For all response calculations, the diffuse augmented def2-SVPD basis set⁷ was used.

Vertical excitation energies and oscillator strengths with the M06-2X⁸ functional were computed with the TURBOMOLE program package⁹ using a quadrature grid of type m4. Solvent effects on the excitation energies were included through the COSMO model¹⁰ ($\epsilon = 8.93$, $n = 1.424$ for CH_2Cl_2). Transition densities for the excitations with high HOMO-1 \rightarrow LUMO character were obtained as described in Ref. 11. The density plots shown in Figure 4b were generated using isosurface values of ± 0.005 .

Vertical excitation energies, oscillator strengths, two-photon absorption cross sections and transition dipole moments between excited states employing the CAM-B3LYP¹² functional were calculated with the LS-DALTON program¹³ using gridsize 4.

Two-photon absorption cross section

The first residue of the quadratic response function can be used to evaluate the elements of the two-photon absorption transition amplitude tensor

$$S_{\alpha\beta} = \sum_{k>0} \left(\frac{\langle 0 | \hat{\mu}_\alpha | k \rangle \langle k | \hat{\mu}_\beta | f \rangle}{\omega_k - \omega_f / 2} + \frac{\langle 0 | \hat{\mu}_\beta | k \rangle \langle k | \hat{\mu}_\alpha | f \rangle}{\omega_k - \omega_f / 2} \right).$$

Here, 0 denotes the ground state, f the final excited state and the sum runs over all excited states k (α and β indicate the Cartesian coordinates x, y, z). The orientationally averaged transition probability for the absorption of two photons with identical energy $\omega_f / 2$ is then given in atomic units by

$$\delta_{2PA}^{au} = \frac{1}{30} \sum_{\alpha,\beta} (F \cdot S_{\alpha\alpha} S_{\beta\beta}^* + G \cdot S_{\alpha\beta} S_{\beta\alpha}^* + H \cdot S_{\alpha\beta} S_{\alpha\beta}^*).$$

For linearly polarized light, $F = G = H = 2$. The conversion to the two-photon absorption cross section in GM units was achieved in the same way as it is done in the DALTON program¹⁴:

$$\delta_{2PA}^{GM} = \frac{(2\pi)^3 \alpha \alpha_0^5 \omega^2}{c \pi I} \delta_{2PA}^{au}.$$

In this equation, α is the fine structure constant, a_0 is the Bohr radius (in cm), c is the speed of light (in cm s⁻¹), ω is the photon energy (in au) and $\pi\Gamma$ is the Lorentzian-shape broadening of the excited state (in au; $\Gamma = 0.1$ eV).

Basis set and functional dependence of the 2PA cross section

For the calculation of the 2PA cross section, the combination of the CAM-B3LYP functional with a basis set containing diffuse functions was found to be promising when compared to coupled cluster quadratic response theory.¹⁵ We have therefore chosen to report CAM-B3LYP/def2-SVPD results in the main manuscript. Nevertheless, we have tested the influence of the basis set and the employed functional.

The vertical excitation energies and oscillator strengths computed with CAM-B3LYP/def2-SVPD are very similar to the ones we obtained at the M06-2X/def2-SVPD+COSMO level (the M06-2X results for the first excitation energy were previously found to be systematically shifted compared to the experimental values²). Neither the excitation energy nor the 2PA cross section is much affected by changing the basis set from def2-SVPD to def2-SVP⁶ (see Table S1).

Table S1. Comparison of computed excitation energies and absorption properties for the def2-SVPD and the def2-SVP basis sets.

| | | CAM-B3LYP/def2-SVPD | | | CAM-B3LYP/def2-SVP | | |
|----------|----------------|---------------------|-----------|---------------------|--------------------|-----------|---------------------|
| Dye | State | VEE (eV) | f_{1PA} | δ_{2PA} (GM) | VEE (eV) | f_{1PA} | δ_{2PA} (GM) |
| 1 | S ₁ | 2.91 | 0.539 | 1.01 | 2.97 | 0.558 | 1.26 |
| | S ₂ | 3.78 | 0.042 | 1.91 | 3.80 | 0.047 | 1.75 |
| | S ₃ | 4.06 | 0.042 | 0.04 | 4.06 | 0.041 | 0.02 |
| 2 | S ₁ | 2.72 | 1.067 | 4.65 | 2.77 | 1.091 | 5.32 |
| | S ₂ | 3.59 | 0.083 | 7.84 | 3.61 | 0.096 | 7.33 |
| | S ₃ | 3.75 | 0.058 | 186.96 | 3.77 | 0.059 | 168.43 |
| 3 | S ₁ | 2.48 | 1.638 | 17.26 | 2.52 | 1.672 | 19.09 |
| | S ₂ | 3.27 | 0.072 | 2128.99 | 3.29 | 0.075 | 1978.16 |
| | S ₃ | 3.41 | 0.266 | 21.11 | 3.44 | 0.309 | 19.45 |
| 4 | S ₁ | 2.52 | 1.254 | 13.40 | 2.56 | 1.272 | 14.86 |
| | S ₂ | 3.33 | 0.067 | 1165.12 | 3.34 | 0.070 | 1072.46 |
| | S ₃ | 3.43 | 0.200 | 12.38 | 3.46 | 0.231 | 11.19 |
| 5 | S ₁ | 2.59 | 1.389 | 11.64 | 2.63 | 1.402 | 13.15 |
| | S ₂ | 3.48 | 0.065 | 876.99 | 3.49 | 0.068 | 816.25 |
| | S ₃ | 3.50 | 0.156 | 12.48 | 3.52 | 0.185 | 11.50 |

We have also done calculations with the B3LYP functional for comparison. We previously found that the excitation energies are not systematically shifted compared to experiment because B3LYP is not properly describing excitations with charge transfer character.² This means that the energy of these excitations is underestimated compared to other excitations which can lead to a different order of the excited states. The character of the first three excitations is found to be the same as for the M06-2X functional (see Table S2). We note however, that for B3LYP the order of the S_2 and S_3 states is reversed for dye **2** and that the energy difference between the S_2 and S_3 states is larger than for M06-2X and CAM-B3LYP (except for dye **2**). The energetics of the excited states, compared to experiment, is thus better described by the M06-2X and CAM-B3LYP functionals.

Table S2. Computed linear optical properties at the B3LYP/def2-SVPD+COSMO level of theory.

| B3LYP/def2-SVPD+COSMO | | | | |
|-----------------------|-------|----------|------------------|-------------------------|
| Dye | State | VEE (eV) | f_{IPA} | contribution |
| 1 | S_1 | 2.81 | 0.605 | 96% H \rightarrow L |
| | S_2 | 3.36 | 0.055 | 97% H-1 \rightarrow L |
| | S_3 | 3.61 | 0.046 | 99% H-2 \rightarrow L |
| 2 | S_1 | 2.54 | 0.954 | 91% H \rightarrow L |
| | S_2 | 3.02 | 0.039 | 98% H-1 \rightarrow L |
| | S_3 | 3.09 | 0.306 | 89% H-2 \rightarrow L |
| 3 | S_1 | 2.08 | 1.246 | 97% H \rightarrow L |
| | S_2 | 2.46 | 0.040 | 98% H-1 \rightarrow L |
| | S_3 | 2.93 | 1.058 | 86% H-2 \rightarrow L |
| 4 | S_1 | 2.16 | 0.987 | 96% H \rightarrow L |
| | S_2 | 2.60 | 0.046 | 98% H-1 \rightarrow L |
| | S_3 | 3.01 | 0.678 | 92% H-2 \rightarrow L |
| 5 | S_1 | 2.29 | 1.103 | 94% H \rightarrow L |
| | S_2 | 2.76 | 0.047 | 99% H-1 \rightarrow L |
| | S_3 | 3.04 | 0.592 | 92% H-2 \rightarrow L |

The absolute values obtained for the 2PA cross section with the B3LYP functional are summarized in Table S3. When comparing these values to the ones obtained with the CAM-B3LYP functional, we find that they sometimes differ considerably. Nevertheless, they show a qualitative agreement regarding the trend and hence they support our discussion and conclusion in the main manuscript: transitions with high HOMO-1 \rightarrow LUMO character show an increasing 2PA cross section for the dyes in the order **1, 2, 5, 4, 3**.

Table S3. Computed linear and nonlinear optical properties at the B3LYP/def2-SVP level of theory.

| B3LYP/def2-SVP | | | | |
|----------------|----------------|----------|------------------|----------------------------|
| Dye | State | VEE (eV) | f_{IPA} | $\delta_{2\text{PA}}$ (GM) |
| 1 | S ₁ | 3.00 | 0.494 | 1.01 |
| | S ₂ | 3.38 | 0.075 | 0.53 |
| | S ₃ | 3.60 | 0.028 | 0.02 |
| 2 | S ₁ | 2.65 | 0.811 | 7.76 |
| | S ₂ | 3.06 | 0.029 | 263.06 |
| | S ₃ | 3.16 | 0.418 | 2.76 |
| 3 | S ₁ | 2.14 | 1.160 | 23.38 |
| | S ₂ | 2.49 | 0.034 | 2789.79 |
| | S ₃ | 3.01 | 1.328 | 22.88 |
| 4 | S ₁ | 2.21 | 0.818 | 15.73 |
| | S ₂ | 2.58 | 0.036 | 1135.13 |
| | S ₃ | 3.11 | 0.815 | 2.34 |
| 5 | S ₁ | 2.35 | 0.941 | 14.63 |
| | S ₂ | 2.76 | 0.036 | 845.06 |
| | S ₃ | 3.12 | 0.751 | 2.55 |

5. References

1. R. P. Sabatini, T. M. McCormick, T. Lazarides, K. C. Wilson, R. Eisenberg, D. W. McCamant, *J. Phys. Chem. Lett.* **2011**, *2*, 223–227.
2. D. K. Kölmel, A. Hörner, J. A. Castañeda, J. A. P. Ferencz, A. Bihlmeier, M. Nieger, S. Bräse, L. A. Padilha, *J. Phys. Chem. C* **2016**, *120*, 4538–4545.
3. C. Xu, W. W. Webb, *J. Opt. Soc. Am. B* **1996**, *13*, 481–491.
4. N. S. Makarov, M. Drobizhev, A. Rebane, *Opt. Express* **2008**, *16*, 4029–4047.
5. A. D. Becke, *J. Chem. Phys.* **1993**, *98*, 5648–5652.
6. F. Weigend, R. Ahlrichs, *Phys. Chem. Chem. Phys.* **2005**, *7*, 3297–3305.
7. D. Rappoport, F. Furche, *J. Chem. Phys.* **2010**, *133*, 134105.
8. Y. Zhao, D. G. Truhlar, *Acc. Chem. Res.* **2008**, *41*, 157–167.
9. TURBOMOLE, Program Package for *ab initio* Electronic Structure Calculations, Version 6.6 (2014), a development of University of Karlsruhe and Forschungszentrum Karlsruhe GmbH, 1989–2007, TURBOMOLE GmbH since 2007; see <http://www.turbomole.com>.
10. A. Klamt, G. J. Schüürmann, *J. Chem. Soc. - Perkin Trans. 2* **1993**, 799–805.
11. J. Chmela, M. E. Harding, D. Matyosek, C. E. Anson, F. Breher, W. Klopper, *ChemPhysChem* **2016**, *17*, 37–45.
12. T. Yanai, D. P. Tew, N. C. Handy, *Chem. Phys. Lett.* **2004**, *393*, 51–57.
13. LS-DALTON, a linear scaling molecular electronic structure program, Release Dalton2015.1 (2015); see <http://daltonprogram.org>.
14. DALTON, a molecular electronic structure program, Release Dalton2015.1 (2015); see <http://daltonprogram.org>.
15. M. J. Paterson, O. Christiansen, F. Pawłowski, P. Jørgensen, C. Hättig, T. Helgaker, P. Sałek, *J. Chem. Phys.* **2006**, *124*, 054322.